ARTICLE
Journal of Cellular Biochemistry 114:428–434 (2013)

Journal of Cellular Biochemistry

Imaging the Efficacy of UVC Irradiation on Superficial Brain Tumors and Metastasis in Live Mice at the Subcellular Level

Masashi Momiyama,[1,2,3] Atsushi Suetsugu,[1] Hiroaki Kimura,[1] Hiroyuki Kishimoto,[1] Ryoichi Aki,[1] Akimitsu Yamada,[3] Harumi Sakurada,[3] Takashi Chishima,[3] Michael Bouvet,[2] Itaru Endo,[3] and Robert M. Hoffman[1,2*]

[1]*AntiCancer, Inc., San Diego, California 92111*
[2]*Department of Surgery, University of California, San Diego, California 92103-8220*
[3]*Department of Gastroenterological Surgery, Yokohama City University, Yokohama, Japan*

ABSTRACT

The effect of UVC irradiation was investigated on a model of brain cancer and a model of experimental brain metastasis. For the brain cancer model, brain cancer cells were injected stereotactically into the brain. For the brain metastasis model, lung cancer cells were injected intracarotidally or stereotactically. The U87 human glioma cell line was used for the brain cancer model, and the Lewis lung carcinoma (LLC) was used for the experimental brain metastasis model. Both cancer cell types were labeled with GFP in the nucleus and RFP in the cytoplasm. A craniotomy open window was used to image single cancer cells in the brain. This double labeling of the cancer cells with GFP and RFP enabled apoptosis of single cells to be imaged at the subcellular level through the craniotomy open window. UVC irradiation, beamed through the craniotomy open window, induced apoptosis in the cancer cells. UVC irradiation was effective on LLC and significantly extended survival of the mice with experimental brain metastasis. In contrast, the U87 glioma was relatively resistant to UVC irradiation. The results of this study suggest the use of UVC for treatment of superficial brain cancer or metastasis. J. Cell. Biochem. 114: 428–434, 2013.

KEY WORDS: GFP; RFP; APOPTOSIS; MITOSIS; SUBCELLULAR DYNAMICS; BRAIN METASTASIS; BRAIN CANCER; MOUSE MODEL; CRANIOTOMY WINDOW; IN VIVO IMAGING

Brain metastasis is often the lethal event in many malignancies including lung cancer, breast cancer and melanoma [Fidler et al., 2002, 2010; Fidler, 2011; Langley and Fidler, 2011]. Both brain cancer and brain metastasis are often treatment-resistant except for surgical resection, which in many instances is incomplete, resulting in recurrence. Better approaches are necessary, especially with regard to lowering the recurrence rate after surgery [Stummer et al., 2006].

Our laboratory pioneered in vivo imaging with fluorescent proteins [Chishima et al., 1997; Yang et al., 2000; Hoffman, 2005]. We have also developed dual-color cancer cells, in which red fluorescent protein (RFP) is expressed in the cytoplasm and green fluorescent protein (GFP), linked to histone H2B, is expressed in the nucleus. Nuclear GFP expression enables visualization of nuclear dynamics including cell cycle events and apoptosis, whereas simultaneous cytoplasmic RFP expression enables visualization of nuclear–cytoplasmic ratios as well as simultaneous cell and nuclear shape changes. Thus, total cellular dynamics can be visualized in the living dual-color cells in real time both in vitro and in vivo [Yamamoto et al., 2004; Yamauchi et al., 2005; Jiang et al., 2006].

With the use of imaging based on GFP expression in cancer cells [Hoffman, 2005], we have observed spontaneous metastasis to the brain in three orthotopic nude mouse model systems of human cancer: the PC-3 human prostate cancer cell line [Yang et al., 1999a]; the LOX human melanoma cell line [Yang et al., 1999b]; and

Abbreviations used: GFP, green fluorescent protein; RFP, red fluorescent protein; LLC, Lewis lung carcinoma; U87, U87 human glioma.

Conflict of interest: None of the authors have a conflict of interest regarding this study.

Grant sponsor: National Cancer Institute; Grant numbers: CA132971, CA142669.

*Correspondence to: Robert M. Hoffman, PhD, AntiCancer Inc., 7917 Ostrow Street, San Diego, CA 92111. E-mail: all@anticancer.com

Manuscript Received: 23 August 2012; Manuscript Accepted: 30 August 2012

Accepted manuscript online in Wiley Online Library (wileyonlinelibrary.com): 7 September 2012

DOI 10.1002/jcb.24381 • © 2012 Wiley Periodicals, Inc.

spinal cord glioma using the U87 human glioma cell line [Hayashi et al., 2009; Hoffman, 2009].

Photodynamic therapy (PDT) has been shown to be effective for certain cancer types [Castano et al., 2006]. UV light has been used for the phototherapy of cutaneous malignancies. Psoralen plus UVA (PUVA) and narrowband UVB were found to be effective [Gilchrest et al., 1976; Hofer et al., 1999; Carter and Zug, 2009]. However, the effect of UV light on cancer cells is not well understood [Zacal and Rainbow, 2007; Benencia et al., 2008; Kim et al., 2008]. UV light has been mainly used for skin cancer, since short wavelength light does not penetrate deeply through the skin [Kimura et al., 2010].

We previously investigated the cell-killing efficacy of UV light on cancer cells expressing GFP in the nucleus and RFP in the cytoplasm (dual-color cells). UV-induced cancer cell death was found to be wave-length and dose dependent, as well as cell-line dependent. For UVC, as little as 25 J/m^2 UVC irradiation killed approximately 70% of the double-labeled cancer cells. UVC exposure also suppressed cancer cell growth in a nude mouse model of minimal residual cancer (MRC). No apparent side effects of UVC exposure were observed [Kimura et al., 2010].

In another previous study, the efficacy of fluorescence-guided UVC irradiation on the growth of murine melanoma expressing GFP in the ear of RFP mice was determined. The GFP-expressing melanoma and RFP-expressing blood vessels from the transgenic mice expressing RFP used as hosts were readily visible using noninvasive imaging. UVC inhibited melanoma growth and also damaged blood vessels in the tumor [Tsai et al., 2010].

Cancer cells with and without fluorescent protein expression were irradiated with various doses of UVC. Lewis lung carcinoma cells (LLC) and U87 human glioma cells expressing GFP in the nucleus and RFP in the cytoplasm and non-colored LLC and U87 cells were irradiated with various doses of UVC. Compared to non-colored LLC and U87 cells, the number of dual-color LLC and U87 cells decreased significantly due to UVC irradiation. These results suggest that expression of fluorescent proteins in cancer cells can enhance PDT using UVC and possibly with other wave lengths of light as well [Momiyama et al., 2012].

The present study determined the efficacy of UVC irradiation on superficial brain cancer and brain metastasis in a nude mouse model that enabled imaging of the cancer cells at the subcellular level in the brain of the live animal.

MATERIALS AND METHODS

CELLS

To establish LLC or U87 human glioma (U87) GFP–RFP cells, the cells were transfected with retroviral RFP and H2B-GFP vectors as previously described [Yamamoto et al., 2004]. LLC or U87 human glioma, cells were transfected with retroviral RFP and H2B–GFP vectors. In brief, the *Hin*dIII/*Not*I fragment from pDsRed2 (Clontech Laboratories, Inc., Palo Alto, CA), containing the full-length RFP cDNA, was inserted into the *Hin*dIII/*Not*I site of pLNCX2 (Clontech Laboratories, Inc.) containing the neomycin resistance gene. PT67, an NIH3T3-derived packaging cell line (Clontech Laboratories, Inc.) expressing the 10 Al viral envelope, was cultured in DMEM (Irvine Scientific, Santa Ana, CA) supplemented with 10% heat-inactivated fetal bovine serum (FBS; Gemini Bio-products, Calabasas, CA). For vector production, PT67 cells, at 70% confluence, were incubated with a precipitated mixture of Lipofectamine reagent (Life Technologies, Inc., Grand Island, NY), and saturating amounts of pLNCX2-DsRed2 plasmid for 18 h. Fresh medium was replenished at this time. The cells were examined by fluorescence microscopy 48 h post-transfection. For selection of a clone producing high amounts of the RFP retroviral vector (PT67-DsRed2), the cells were cultured in the presence of 200–1,000 μg/ml G418 (Life Technologies, Inc.), increased stepwise over 7 days [Hoffman and Yang, 2006a,b,c].

The histone H2B gene has no stop codon, thereby enabling the ligation of the H2B gene to the 5′-coding region of the GFP gene (Clontech Laboratories, Inc.). The histone H2B-GFP fusion gene was then inserted at the *Hin*dIII/ClaI site of the pLHCX (Clontech Laboratories, Inc.) that has the hygromycin resistance gene. To establish a packaging cell clone producing high amounts of the histone H2B-GFP retroviral vector, the pLHCX histone H2B-GFP plasmid was transfected in PT67 cells using the same methods described above for PT67-DsRed2. The transfected cells were cultured in the presence of 200–400 μg/ml hygromycin (Life Technologies, Inc.) increased stepwise over 7 days [Hoffman and Yang, 2006b].

In order to obtain cancer cells expressing both RFP and H2B-GFP, 70% confluent LLC or U87 cells were used. To establish dual-color cells, clones of these cells expressing RFP in the cytoplasm were initially established. In brief, cells were incubated with a 1:1 precipitated mixture of retroviral supernatants of PT67-RFP cells and RPMI 1640 (Irvine Scientific, Santa Ana, CA) containing 10% FBS for 72 h. Fresh medium was replenished at this time. Cells were harvested with trypsin/EDTA 72 h post-transduction and subcultured at a ratio of 1:15 in selective medium, which contained 200 μg/ml of G418. The level of G418 was increased stepwise up to 800 μg/ml [Hoffman and Yang, 2006b].

For establishing dual-color cancer cells, RFP-expressing cells were then incubated with a 1:1 precipitated mixture of retroviral supernatants of PT67 H2B-GFP cells and culture medium. To select the double transformants, cells were incubated with hygromycin 72 h after transfection. The level of hygromycin was increased stepwise from 200 to 800 μg/ml [Hoffman and Yang, 2006b].

Dual-color LLC or U87 cells were maintained in DMEM medium (Hyclone Laboratories, Logan, UT) supplemented with 10% fetal bovine serum (FCS; Hyclone Laboratories). The cells were incubated at 37°C in a humidified atmosphere of 5% CO_2 in air. The cells were collected after trypsinization and stained with trypan blue (Sigma). Only viable cells were counted with a hemocytometer (Hausser Scientific, Horsham, PA).

ANIMALS

Athymic NCR nude mice (*nu*/*nu*), 4–6 weeks of age, were used in this study. Mice were bred and maintained in a barrier facility under HEPA filtration at AntiCancer Inc. (San Diego, CA). Mice were fed with an autoclaved laboratory rodent diet. All animal studies were conducted in accordance with the principals and procedures outlined in the NIH Guide for the Care and Use of Laboratory Animals under assurance number A3873-1.

CRANIOTOMY OPEN WINDOW

Mice were anesthetized with a ketamine mixture (10 μl ketamine HCl, 7.6 μl xylazine, 2.4 μl acepromazine maleate, and 10 μl H_2O) via s.c. injection. After fixing the mice in a prone position, a 1.5 cm incision was made directly down the midline of the scalp. The scalp was retracted and the skull was exposed. Using a skin biopsy punch (Acuderm Inc., Ft. Lauderdale, FL), a 4 mm diameter craniotomy was made over the right parietal bone. The bone fragment was removed carefully in order not to injure the meninges and brain tissue. The craniotomy open window was covered only by the scalp. Thus, only scalp retraction was needed in order to image single cancer cells in the brain. The incision was then closed with a 6-0 surgical suture (ETHICON, Inc., Somerville, NJ). All mice were kept in an oxygenated warmed chamber until they recovered from anesthesia.

INTERNAL CAROTID ARTERY INJECTION OF CANCER CELLS

Mice were anesthetized with a ketamine mixture via s.c. injection. The mice were then fixed on a board with rubber bands in a supine position. A thermo plate (Olympus Corp., Tokyo, Japan) was put on the board in order to maintain constant body temperature throughout the experiment. After the neck was sterilized using 70% ethanol, a 2.0 cm longitudinal incision was made in the skin at the center of the neck. The artery was exposed by blunt dissection from the common carotid artery at the point of division into the internal and external carotid arteries. After the external artery was clamped, dual-color LLC cells (1×10^6 in 20 μl) were slowly injected with a 31-gauge needle into the right internal carotid artery. Immediately after injection, the injected site was pressed with a swab to prevent bleeding or leakage of injected tumor cells. The skin was closed with a 5-0 surgical suture (ETHICON, Inc., Somerville, NJ).

STEREOTACTIC INJECTION OF CANCER CELLS IN THE BRAIN

The mice were anesthetized with a ketamine mixture via s.c. injection. For the superficial brain tumor model, 0.2 μl, containing 2×10^4 dual-color LLC cells, was injected stereotactically at the middle of the craniotomy open window to a depth of 0.1 mm, using a 10 μl Hamilton syringe.

FLUORESCENCE IMAGING

The OV100 Small Animal Imaging System (Olympus Corp., Tokyo, Japan), containing an MT-20 light source (Olympus Biosystems, Planegg, Germany) and DP70 CCD camera (Olympus), was used for imaging live mice [Yamauchi et al., 2006]. The FluoView FV1000 confocal laser microscope (Olympus Corp., Tokyo, Japan) was used for ex vivo imaging. High-resolution images were captured directly on a personal computer (Fujitsu Siemens Computers, Munich, Germany). Images were analyzed with the use of Cell® software (Olympus Biosystems).

UV IRRADIATION

For in vivo UV irradiation, a customized UVC pen light (UVP) was used. The pen light consists of a quartz bulb filled with argon and mercury vapor, which emits primarily at 254 nm (UVC wavelength) encased in an aluminum cylinder. The average output power was measured at 370 mW/cm^2 at the opening of the cylinder [Kimura et al., 2010].

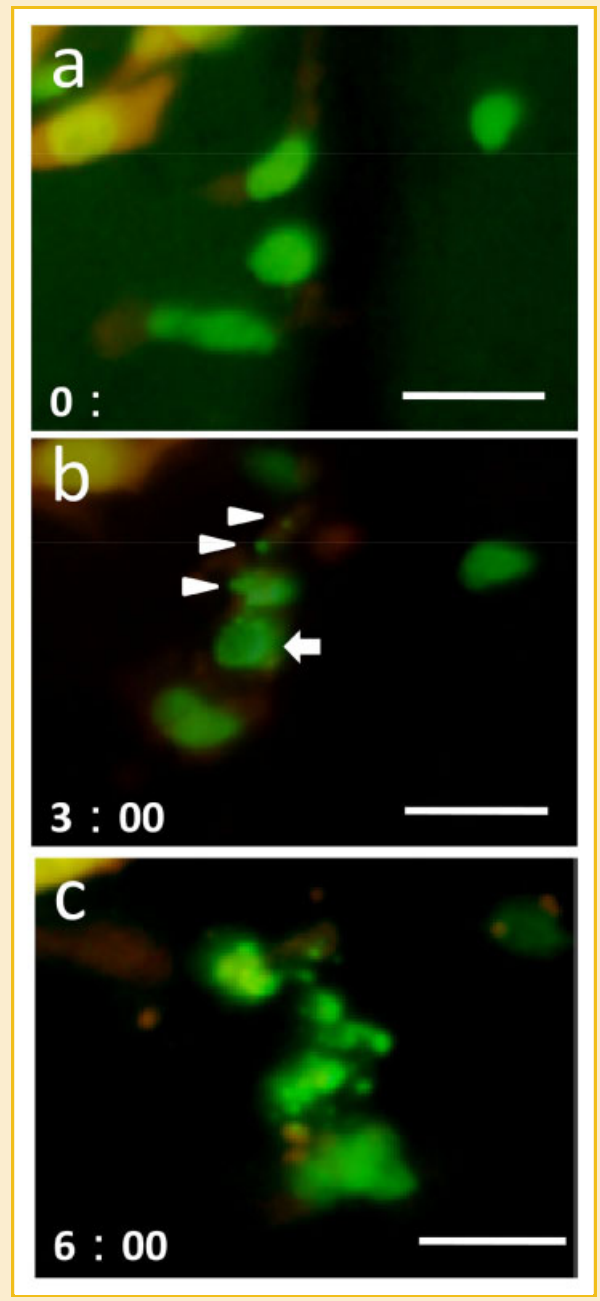

Fig. 1. Real-time imaging of apoptotic cell death in the brain in live mice. a: Seven days after dual-color LLC cell inoculation via the internal carotid artery, the cells were irradiated for 60 s with UVC. b: Three hours after irradiation, aggregation of chromatin at the nuclear membrane (arrow) and fragmented nuclei (arrow heads) were observed. c: Six hours after irradiation, the nuclei appeared to form numerous additional fragments and destruction of RFP-expressing cytoplasm was observed (scale bars, a,b: 100 μm; c: 20 μm).

STATISTICAL ANALYSIS

The experimental data are expressed as the mean ± SD. Statistical analysis was performed using the Student's *t*-test or the

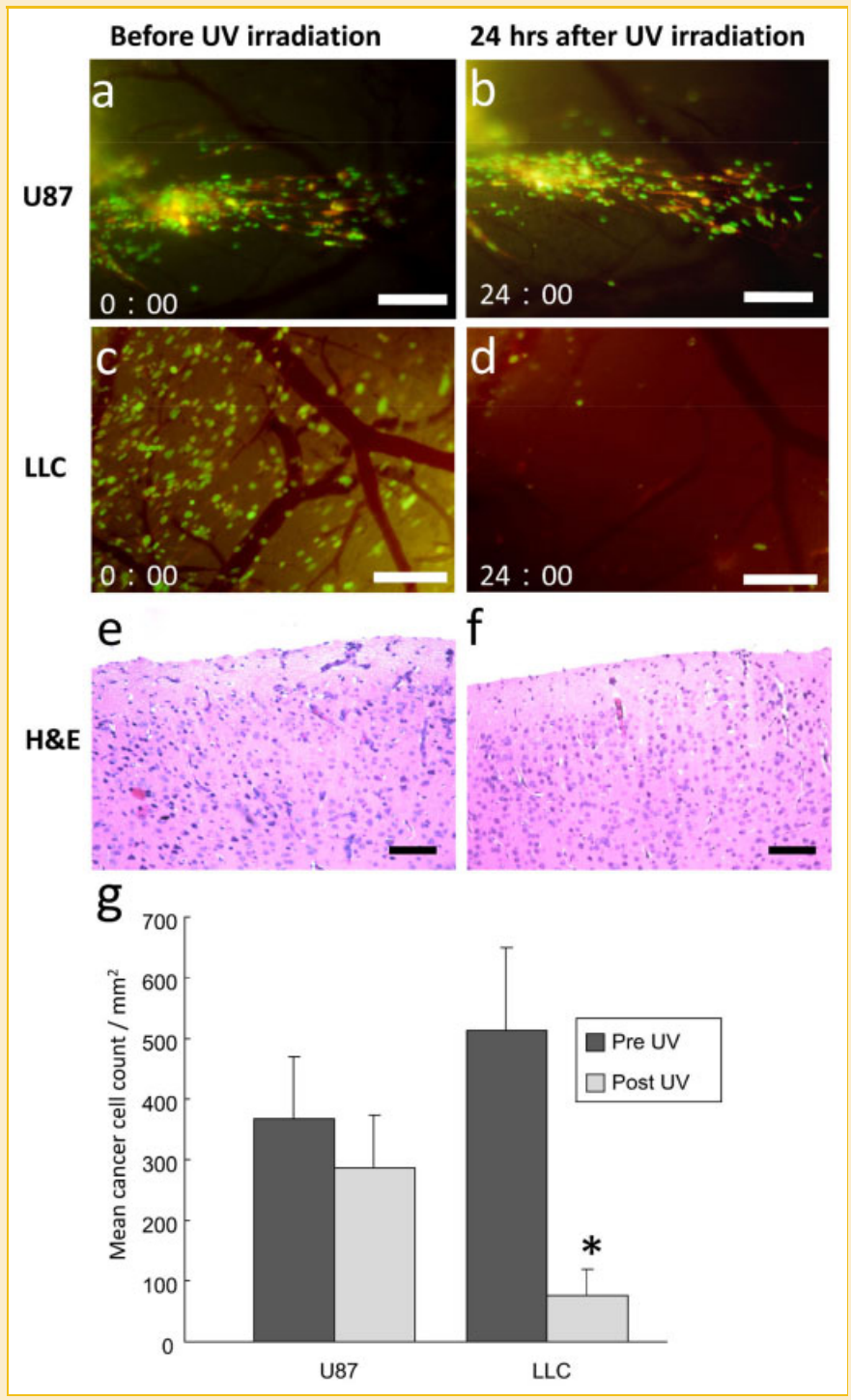

Fig. 2. Cytoxic efficacy of UVC light on dual-color U87 and LLC cells in the brain. a–d: Imaging cytoxic efficacy of UVC irradiation on cancer cells in live mice in the brain. Seven days after inoculation, cells were irradiated for 120 s with UVC light through the craniotomy open window. U87 cells were injected stereotactically and LLC cells were injected via the internal carotid artery. Dual-color U87 cells and LLC cells were observed before and 24 h after irradiation with UVC light. a,b: More than 80% of U87 cells survived UVC irradiation. c,d: More than 90% of the LLC cells died and disappeared after UVC irradiation. No hemorrhage was observed and the blood vessels were not destroyed after irradiation. e,f: Histology of the normal brain surroundings before (e) and 24 h (f) after UVC irradiation. Brain tissue sections obtained from under the craniotomy open window were processed with Hematoxylin and Eosin (H&E) staining. Brain damage after irradiation could not be detected from the histological findings. g: Although there was no significant difference between before and after irradiation in the number of U87 cells ($P = 0.570$), the number of LLC cells in the brain decreased significantly due to UVC irradiation ($^{*}P = 0.003$). Five mice were used in each cell line for this experiment. The experimental data are expressed as the mean ± SD. Statistical analysis was performed using the Student's *t*-test (scale bars: a–d, 200 μm and e–f, 100 μm).

TABLE I. Cytoxic Efficacy of UVC Light on Dual Color U87 and LLC Cells in the Brain

	Pre-UV irradiation cancer (cells/mm^2)	Post-UV irradiation cancer (cells/mm^2)
U87	368.0 ± 243.7	286.3 ± 188.1
LLC	562.5 ± 261.2	79.33 ± 74.61*

Seven days after inoculation, cells were irradiated for 120 s with UVC light through the craniotomy open window. Dual-color U87 cells and LLC cells were observed before and 24 h after irradiation with UVC light. Although there was no significant difference between before and after irradiation in the number of U87 cells ($P = 0.570$), the number of LLC cells in the brain decreased significantly due to UVC irradiation. More than 86% of the LLC cells died after irradiation. Five mice were used in each cell line in this experiment. The experimental data are expressed as the mean ± SD. Statistical analysis was performed using the Student's *t*-test.
*Statistically significant versus pre-UV irradiation ($P = 0.003$).

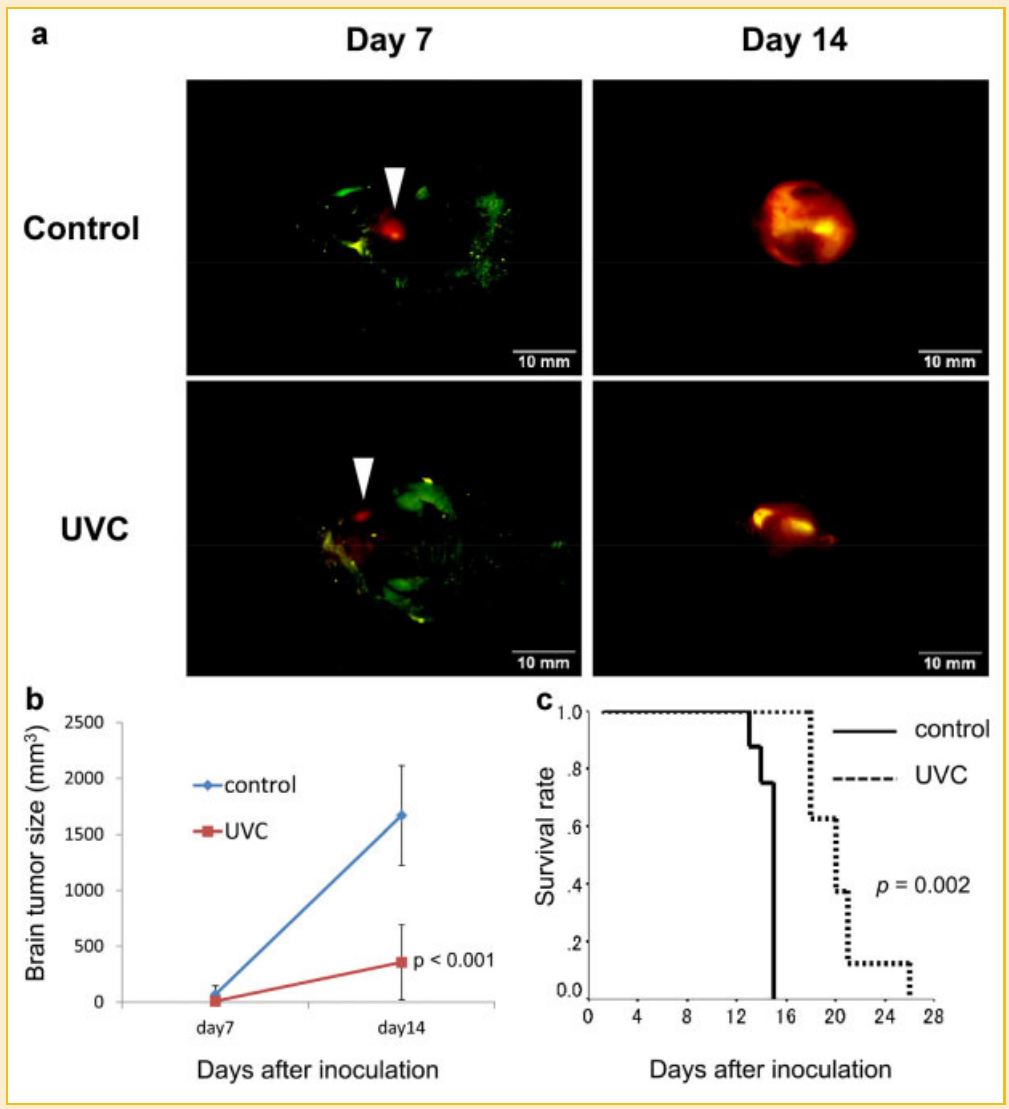

Fig. 3. Efficacy of UVC on dual-color LLC tumor growth in a superficial brain-tumor model. a: Representative images of dual-color LLC tumor growth in untreated mice (control) and mice treated with UVC irradiation (UVC), on Days 7 and 14 after tumor inoculation, are shown (scale bars: 10 mm). Dual-color LLC cells were injected stereotactically to a depth of 0.1 mm in the brain. b: The tumor volumes of UVC irradiated mice and untreated mice (as a control) were compared. Tumor volume in the control group was 4.7-fold larger than in the UVC group (at Day 14, $P < 0.0001$). Eight mice were used in each group. The experimental data are expressed as the mean ± SD. Statistical analysis was performed using the Student's *t*-test (*P*-values: Day 7, 0.073 and Day 14, <0.001). c: Treatment with UVC irradiation significantly prolonged survival in mice with dual-color LLC brain tumors. UVC irradiation was initiated 1 day after cancer cell inoculation and tumors were irradiated for 120 s on Days 1, 4, 7, and 10. Median survival increased from 14.63 days in the control group to 20.25 days (39.0% longer survival) in mice treated with UVC ($P = 0.002$).

Kruskal–Wallis test. Kaplan–Meier analysis with a log-rank test was used to determine survival and difference between treatment groups. A P-value of <0.05 indicated a significant difference.

RESULTS

After UVC irradiation, progressive fragmentation of the GFP-expressing nuclei of dual-color LLC cells in the brain was imaged (Fig. 1). Three hours after irradiation, aggregation of chromatin at the nuclear membrane and fragmentation of the nuclei were observed (Fig. 1b). Six hours after irradiation, the nuclei became more fragmented and destruction of RFP-expressing cytoplasm was observed (Fig. 1c). UVC-induced apoptosis was observed up to a depth of 40 μm in the brain.

COMPARISON OF CYTOXIC EFFICACY OF UVC IRRADIATION ON LLC AND U87 CELLS IN THE BRAIN IN LIVE MICE

Twenty-four hours after UVC light irradiation, the number of LLC cells in the brain decreased significantly. Approximately 86% of LLC cells irradiated with UVC light died and disappeared (Fig. 2c,d,g and Table I). In contrast, the number of U87 cells in the brain was not significantly different before and after UVC irradiation (Fig. 2a,b,g and Table I). No hemorrhage was observed and the blood vessels were not destroyed after irradiation. Furthermore, no apparent brain damage after UVC irradiation was observed from histological findings (Fig. 2e,f) or from the behavior of the mice. UVC irradiation did not appear to affect mouse well-being.

EFFICACY OF UVC THERAPY IN A SUPERFICIAL BRAIN TUMOR MODEL WITH DUAL-COLOR LLC CELLS

Efficacy of UVC therapy in the superficial brain tumor model is shown in Figure 3. Dual-color LLC cells were injected stereotactically into the brain to a depth of 0.1 mm. Tumors were irradiated via the craniotomy window with UVC for 120 s on Days 1, 4, 7, and 10 after cancer cell inoculation. In the control group, tumor size on Day 7 was 68.0 mm^3 and on Day 14, 1,669 mm^3. In the UVC group, on Day 7, the tumor size was 9.33 mm^3 and on Day 14, 356 mm^3. At Day 14 after cancer cell inoculation, tumor volume in the control group was 4.7-fold larger than in the UVC group ($P<0.0001$, Fig. 3a,b).

In a survival study, death from disease was rapid in untreated mice, which had a median survival of 14.6 days. Irradiation of UVC prolonged survival compared with control, increasing the median survival to 20.3 days and that improving survival by 39% ($P=0.002$, Fig. 3c).

DISCUSSION

In the current study, two models were developed: an orthotopic brain cancer model with stereotactic injection of U87 glioma cells and an experimental metastasis model with intra-carotid injection of LLC cells.

In contrast to U87 glioma cells, which were resistant to UVC in vivo, most LLC cells irradiated with UVC died and disappeared in the brain (Fig. 2c,d,g and Table I). Although some of the blood vessels shrank after irradiation, the blood vessels were not destroyed. Additional damage to the normal brain surroundings was not detected histologically (Fig. 2e,f). This result suggested that UVC light has sufficient high energy to kill sensitive cancer cells on the surface of the brain with limited side effects.

UVC light does not deeply penetrate tissue (up to depth of 40 μm) and was not able to kill all of the cancer cells in the brain. Cancer cells deeper than 40 μm could continue growing. UVC light, however, could be of potential use to sterilize the surgical bed after tumor resection. To clarify the effect of UVC light on the cancer cells or at near the surface of the brain, we used a superficial brain tumor model with dual-color LLC cells and irradiated the superficial tumors with UVC light. UVC light therapy inhibited tumor growth and prolonged survival compared with untreated mice. Therefore, cancer cells at the surface of the brain, for example minimal residual cancer after surgical resection, would be a good target for UVC light treatment without serious damage of normal brain tissue.

We have previously shown that fluorescent-protein-expressing dual-color cancer cells were more sensitive to UVC light than non-colored cancer cells [Momiyama et al., 2012]. Therefore UVC light may be a powerful tool for treatment of cancer cells expressing fluorescent reporters which now can be introduced selectively to cancer cells in vivo [Kishimoto et al., 2009].

REFERENCES

Benencia F, Courrèges MC, Coukos G. 2008. Whole tumor antigen vaccination using dendritic cells: Comparison of RNA electroporation and pulsing with UV-irradiated tumor cells. J Transl Med 6:21.

Carter J, Zug KA. 2009. Phototherapy for cutaneous T-cell lymphoma: Online survey and literature review. J Am Acad Dermatol 60:39–50.

Castano AP, Liu Q, Hamblin MR. 2006. A green fluorescent protein-expressing murine tumour but not its wild-type counterpart is cured by photodynamic therapy. Br J Cancer 94:391–397.

Chishima T, Miyagi Y, Wang X, Yamaoka H, Shimada H, Moossa AR, Hoffman RM. 1997. Cancer invasion and micrometastasis visualized in live tissue by green fluorescent protein expression. Cancer Res 57:2042–2047.

Fidler IJ. 2011. The role of the organ microenvironment in brain metastasis. Semin Cancer Biol 21:107–112.

Fidler IJ, Yano S, Zhang RD, Fujimaki T, Bucana CD. 2002. The seed and soil hypothesis: Vascularisation and brain metastases. Lancet Oncol 3:53–57.

Fidler IJ, Balasubramanian K, Lin Q, Kim SW, Kim SJ. 2010. The brain microenvironment and cancer metastasis. Mol Cells 30:93–98.

Gilchrest BA, Parrish JA, Tanenbaum L, Haynes HA, Fitzpatrick TB. 1976. Oral methoxsalen photochemotherapy of mycosis fungoides. Cancer 38: 683–689.

Hayashi K, Yamauchi K, Yamamoto N, Tsuchiya H, Tomita K, Bouvet M, Wessels J, Hoffman RM. 2009. A color-coded orthotopic nude-mouse treatment model of brain-metastatic paralyzing spinal cord cancer that induces angiogenesis and neurogenesis. Cell Prolif 42:75–82.

Hofer A, Cerroni L, Kerl H, Wolf P. 1999. Narrowband (311-nm) UV-B therapy for small plaque parapsoriasis and early-stage mycosis fungoides. Arch Dermatol 135:1377–1380.

Hoffman RM. 2005. The multiple uses of fluorescent proteins to visualize cancer in vivo. Nat Rev Cancer 5:796–806.

Hoffman RM. 2009. Comment re: Preclinical model of spontaneous melanoma metastasis. Cancer Res 69:719.

Hoffman RM, Yang M. 2006a. Subcellular imaging in the live mouse. Nat Protoc 1:775–782.

Hoffman RM, Yang M. 2006b. Color-coded fluorescence imaging of tumor–host interactions. Nat Protoc 1:928–935.

Hoffman RM, Yang M. 2006c. Whole-body imaging with fluorescent proteins. Nat Protoc 1:1429–1438.

Jiang P, Yamauchi K, Yang M, Tsuji K, Xu M, Maitra A, Bouvet M, Hoffman RM. 2006. Tumor cells genetically labeled with GFP in the nucleus and RFP in the cytoplasm for imaging cellular dynamics. Cell Cycle 5:1198–1201.

Kim SC, Park S-S, Lee YJ. 2008. Effect of UV irradiation on colorectal cancer cells with acquired TRAIL resistance. J Cell Biochem 104:1172–1180.

Kimura H, Lee C, Hayashi K, Yamauchi K, Yamamoto N, Tsuchiya H, Tomita K, Bouvet M, Hoffman RM. 2010. UV light killing efficacy of fluorescent protein-expressing cancer cells in vitro and in vivo. J Cell Biochem 110: 1439–1446.

Kishimoto H, Zhao M, Hayashi K, Urata Y, Tanaka N, Fujiwara T., et al. 2009. In vivo internal tumor illumination by telomerase-dependent adenoviral GFP for precise surgical navigation. Proc Natl Acad Sci USA 106:14514–14517.

Langley RR, Fidler IJ. 2011. The seed and soil hypothesis revisited—The role of tumor–stroma interactions in metastasis to different organs. Int J Cancer 128:2527–2535.

Momiyama M, Suetsugu A, Kimura H, Kishimoto H, Aki R, Yamada A, Sakurada H, Chishima T, Bouvet M, Bulgakova NN, Endo I, Hoffman RM. 2012. Fluorescent proteins enhance UVC PDT of cancer cells. Anticancer Res 32:4327–4330.

Stummer W, Pichlmeier U, Meinel T, Wiestler OD, Zanella F, Reulen HJ, ALA-Glioma Study Group. 2006. Fluorescence-guided surgery with 5-aminolevulinic acid for resection of malignant glioma: A randomised controlled multicentre phase III trial. Lancet Oncol 7:392–401.

Tsai M-H, Aki R, Amoh Y, Hoffman RM, Katsuoka K, Kimura H, Lee C, Chang CH. 2010. GFP-fluorescence-guided UVC irradiation inhibits melanoma growth and angiogenesis in nude mice. Anticancer Res 30:3291–3294.

Yamamoto N, Jiang P, Yang M, Xu M, Yamauchi K, Tsuchiya H, Tomita K, Wahl GM, Moossa AR, Hoffman RM. 2004. Cellular dynamics visualized in live cells in vitro and in vivo by differential dual-color nuclear-cytoplasmic fluorescent-protein expression. Cancer Res 64:4251–4256.

Yamauchi K, Yang M, Jiang P, Yamamoto N, Xu M, Amoh Y, Tsuji K, Bouvet M, Tsuchiya H, Tomita K, Moossa AR, Hoffman RM. 2005. Real-time in vivo dual-color imaging of intracapillary cancer cell and nucleus deformation and migration. Cancer Res 65:4246–4252.

Yamauchi K, Yang M, Jiang P, Xu M, Yamamoto N, Tsuchiya H, Tomita K, Moossa AR, Bouvet M, Hoffman RM. 2006. Development of real-time subcellular dynamic multicolor imaging of cancer-cell trafficking in live mice with a variable-magnification whole-mouse imaging system. Cancer Res 66:4208–4214.

Yang M, Jiang P, Sun FX, Hasegawa S, Baranov E, Chishima T, Shimada H, Moossa AR, Hoffman RM. 1999a. A fluorescent orthotopic bone metastasis model of human prostate cancer. Cancer Res 59:781–786.

Yang M, Jiang P, An Z, Baranov E, Li L, Hasegawa S, Al-Tuwaijri M, Chishima T, Shimada H, Moossa AR, Hoffman RM. 1999b. Genetically fluorescent melanoma bone and organ metastasis models. Clin Cancer Res 5:3549–3559.

Yang M, Baranov E, Jiang P, Sun F-X, Li X-M, Li L, Hasegawa S, Bouvet M, Al-Tuwaijri M, Chishima T, Shimada H, Moossa AR, Penman S, Hoffman RM. 2000. Whole-body optical imaging of green fluorescent protein-expressing tumors and metastases. Proc Natl Acad Sci USA 97:1206–1211.

Zacal N, Rainbow AJ. 2007. Photodynamic therapy resistant human colon carcinoma HT29 cells show cross-resistance to UVA but not UVC Light. Photochem Photobiol 83:730–737.